Control Design for Future Agile Fighters

Patrick C. Murphy and John B. Davidson
NASA Langley Research Center
Hampton, Virginia

AIAA Paper No. 91-2882

Presented at the 1991 Atmospheric Flight Mechanics Conference

New Orleans, Louisiana
August 12-14, 1991

CONTROL DESIGN FOR FUTURE AGILE FIGHTERS

Patrick C. Murphy, NASA Langley Research Center, Hampton, Virginia *

John B. Davidson, NASA Langley Research Center, Hampton, Virginia *

Abstract

The CRAFT control design methodology is presented. CRAFT stands for the design objectives addressed, namely, Control power, Robustness, Agility, and Flying Qualities Tradeoffs. The approach combines eigenspace assignment, which allows for direct specification of eigenvalues and eigenvectors, and a graphical approach for representing control design metrics that captures numerous design goals in one composite illustration. The methodology makes use of control design metrics from four design objective areas, namely, control power, robustness, agility, and flying qualities. An example of the CRAFT methodology as well as associated design issues are presented. Control design metrics are evaluated for systematic eigenvalue placements over the complex plane. Metric surfaces are formed by plotting metric values for each of the frequency and damping points specified. Graphical overlays of the metric surfaces are then used to show the best design compromise for a variety of design criteria. Since the sensitivity of the metrics to pole placement is clearly displayed, the designer can assess the cost of tradeoffs. This approach enhances the designer's ability to make informed design tradeoffs and to reach effective final designs.

Symbols

A	plant matrix
B	control distribution matrix for states
C	state distribution matrix for outputs
D	control distribution matrix for outputs
E	uncertainty model
g	feedback gain
G	feedback gain matrix
GM	gain metric based on sum of squares of gains
I	identity matrix
K	plant compensation
KG	loop transfer matrix
L	matrix defining achievable subspace for ν
M	state distribution matrix for measurements
m	number of controls
N	control distribution matrix for measurements
n	number of states
p	number of outputs
q	pitch rate, rad/sec.
r	number of measurements
s	Laplace variable, $s=j\omega$
T	scale matrix
U	control vector (mx1)
V	matrix of eigenvectors
V_o	trim velocity, fps.
w	desired eigenvector projection vector
W	matrix of w_i columns
X	state vector (nx1)
Y	output vector (px1)
Z	measurement vector (rx1)
α	angle of attack, rad.
λ	eigenvalue
θ	pitch angle, rad.
ν	eigenvector
s	singular value
ω	frequency, rad/sec
ζ	damping ratio

subscripts

a	achievable values
c	associated with controller
d	desired values
i	index over n modes
p	associated with pilot
s	scaled vector or matrix
ss	steady state

Introduction

Advances in weapons and aircraft technology are significantly changing air combat. In the past, air combat engagements often resulted in tail chase fights measured in minutes, now they are measured in seconds with combatants using all-aspect weapons. New control effectors, such as thrust vectoring and retractable nose strakes, offer the capability to expand the flight envelope with greater control than previously obtainable. Success in the fighter combat arena of the future will demand increased capability from aircraft technology. Future fighters may have to operate in environments where having enhanced maneuverability and controllability, throughout a greatly expanded flight envelope, including high angle of attack, is a requirement. Studies involving piloted and numerical air combat simulations [refs.1-6] have shown that fighters with this capability are able to perform combat maneuvers in shorter time and in less space and thus achieve a tactical advantage.

To achieve high levels of enhanced maneuverability and controllability or agility, as well as post-stall maneuvering capability, requires successful development and integration of several emerging technologies (ref.7). This study focuses on the problem of designing control laws for enhanced agility and supermaneuverability. This research has been conducted in two phases. The first phase efforts focused on characterizing an aircraft's agility. Although many agility

* Aerospace Engineer, Member AIAA

metrics have been proposed [8-15], in general their primary purpose is for assessing combat capability and do not readily lend themselves to be used in the control design process. The first phase efforts have been reported in reference 16 and have resulted in a candidate set of control design agility metrics that may prove useful to a flight control law designer. In general, control design metrics are quantitative measures of specific system capabilities that translate desired operational characteristics into useful engineering terms for the control designer. The second and current phase of research is concentrating on the development of a design methodology for enhanced agility utilizing the control design agility metrics. Designing for enhanced agility represents a serious challenge to the flight controls engineer, since the final design is always a compromise among many opposing tradeoffs. Besides agility, other areas also require demanding design tradeoffs that cannot be ignored in the design. Other key areas are flying qualities (characterizing pilot-in-the-loop demands), robustness (characterizing system tolerance to model error), and control power (characterizing control effector requirements or limits). Each of the four areas contain many design metrics; some represent hard design constraints that must be met and many vary with flight condition. This paper reports on the initial development work that has been done to develop a flight control design methodology and design criteria that allow a designer to make informed tradeoffs among many different and often competing requirements.

Design Approach

The design approach is referred to as CRAFT which stands for the design objectives addressed, namely, Control power, Robustness, Agility, and Flying Qualities Tradeoffs. This approach provides the designer with a graphical tool to simultaneously assess metrics from the four design objective areas. The strength of this approach comes from the use of eigenspace assignment, which allows direct specification of eigenvalues and eigenvectors in the design, in combination with graphical overlays of metric surfaces which capture the design goals in a composite illustration. In this approach, design tradeoffs are made by interpreting graphical overlays of metric surfaces that quantitatively characterize each design goal. Numerous metrics can be applied simultaneously from each of the four design objective areas or any area for which metrics can be expressed in engineering terms. Graphical overlays of the metric surfaces show the best design compromise for all the design criteria and display the "cost" of changing from that design point. This can greatly enhance the designer's ability to make informed design tradeoffs.

CRAFT is summarized in block diagram form in figure 1. The design process begins by selecting a reasonable range of frequency and damping for the closed-loop dynamics of interest. For example, if a longitudinal design was desired, a range of frequency and damping for the short-period mode would be selected with the phugoid mode specified to meet Level 1 flying qualities. Within this range, a grid of design points is chosen to systematically cover the space. Some metrics may be known before the closed-loop design, such as flying qualities specifications. However, the control power, robustness, and agility metrics require determination of the closed-loop system. Using eigenspace assignment as the control design algorithm, feedback gains are computed to achieve the desired placement of the eigenvalues for the closed-loop system at each design point. With eigenspace assignment, the designer also must define eigenvectors; specifying the eigenvectors is discussed in Design Issues. Once the desired closed-loop systems are determined for a desired set of frequency (ω) and damping (ζ) pairs, each control design metric can be evaluated and plotted producing a surface over the ζ–ω space. Viewing the metric surface in a 2-D contour plot highlights the most desirable region to locate the short period pole with respect to the particular metric studied. The individual metric surfaces are an indication of the sensitivity of that metric to closed-loop pole location. A final overlay plot of desirable regions from each metric surface can then be obtained. This is represented by the bottom-center block of figure 1. The intersection of desirable regions provide the best design compromise for all the design criteria considered. Often desirable regions may not overlap and some compromise will be required. For example, the designer may feel it necessary to give up Level 1 flying qualities to achieve acceptable robustness margins. With graphical overlays of metric surfaces the designer is given a method to make design tradeoffs in light of the relative "cost" of the tradeoffs being made. The designer can assess the cost of tradeoffs, since the sensitivity of the metrics to pole placement is clearly displayed. Although many metrics can be used, the designer has the opportunity to select or emphasize certain design metrics, such as agility, to achieve a desired final effect.

Control Design Metrics

Control design metrics are an integral part of CRAFT. Many control design metrics exist for aircraft and most fit into one of the four design objective areas discussed above. In this paper a representative metric is proposed for each design objective area. As experience is gained with the methodology, these metrics and other metrics will be tuned to provide greater sensitivity to design goals and designer needs.

Control Power Metrics

Metrics in the first design objective area characterize control power or control power required. Control power metrics provide measures of the forces and moments acting on an aircraft. The metric chosen for this paper is based on a Euclidean norm of gains and indirectly represents a measure of control power required to achieve each desired pole location. In addition, the specification made for the other eigenvalues and eigenvectors is also reflected. The assumption is made that larger gains generally correspond to a demand for greater control deflection or deflection rate and this, in turn, reflects a demand for greater control

power. For this metric smaller values are more desirable since small gains reflect reduced control power demands. The expression for the gain metric is given as

$$GM(\zeta,\omega) = \frac{gm(\zeta,\omega)}{\max\limits_{(\zeta,\omega)} gm(\zeta,\omega)} \qquad (1)$$

where

$$gm(\zeta,\omega) = \sqrt{\sum_{i=1}^{m}\sum_{j=1}^{n} g^2_{ij}(\zeta,\omega)}$$

which is the square root of the sum of squares of gains normalized by the maximum gain over all design points. If desired, a weighting matrix to selectively emphasize or eliminate certain gains from the analysis could be included.

Robustness Metrics

The next design objective area of interest is multivariable stability robustness. An important concern to control designers is that the control system can tolerate the inevitable model error associated with mathematical descriptions of physical systems. Model error has several sources but certainly one source of concern is the limited ability of linear math models to represent the real aircraft. Strong nonlinearities exist in the aerodynamic model at high angles of attack and for fighter aircraft inertial roll coupling is an additional issue. Therefore, robustness is an especially important design consideration for high angle of attack and high agility aircraft.

A variety of metrics can be used to indicate the regions in $\zeta-\omega$ space with the greatest tolerance to model error. For initial designs, unstructured uncertainties, in the form of multiplicative error models at the input and output, are suggested. For a given error model, singular values of the inverse return difference matrix provide an easily computed and general robustness metric. Structured uncertainties would provide less conservative measures for configuration specific cases, however much more computation and user knowledge of uncertainities are involved. Although more conservatism than probably desired is obtained with unstructured uncertainty models, some benefit is obtained by erring on the conservative side for initial designs. The more conservative metric yields a smaller desirable region in the ζ-ω space, therefore the designer has some confidence that being on or near the edge of that region is not prohibitive.

This candidate metric is determined from the minimum singular value given as $\underline{\sigma}[I + (KG)^{-1}]$, where KG is the loop transfer matrix. An important consideration in using these metrics is that the peaks do not represent regions of guaranteed stability. They are regions with the most promise for robustness over the $\zeta-\omega$ space considered. If an uncertainty model, E(s), were available, it could be applied to determine the regions of guaranteed stability. A sufficient condition for stability is (ref. 17)

$$\underline{\sigma}[I + (K(s)G(s))^{-1}] > \bar{\sigma}[E(s)] \qquad \text{for } s=j\omega \qquad (2)$$

Since an uncertainty model is not always conveniently available, this metric was chosen to highlight the regions with the most promise. It is possible to show that metric values of 0.5 correspond to a multivariable equivalent of 6 db gain margin and 30^o phase margin (see ref. 17). Therefore, it is reasonable to view regions of the robustness metric with values greater than 0.5 to be desirable regions.

Agility Metrics

A third design objective area of interest is agility. Agility in this study is restricted to airframe agility; the agility metrics, unlike many in the literature, do not reflect pilot compensation effects. This was done intentionally to allow separation of flying qualities and agility metrics. This approach enhances a "building block" design philosophy where the designer can choose to add or delete varying degrees of any characteristic by selecting the appropriate metrics. Thus, design freedom exists within regions of Level 1 flying qualities (or Level 2 if Level 1 cannot be achieved) to select the desired level of airframe agility. The agility metrics in combination with the flying qualities metrics aid the designer in selecting the most agile aircraft within the capabilities of a pilot.

Some controversy exists on the exact definition of agility and which parameters best describe it (ref. 18). This reflects the limited experience of both the operational and research community with advanced agile fighters. A significant experience base is needed with advanced concepts involving air combat with high-α flight, thrust vectoring, all aspect weapons, etc. before precise definitions will finally be agreed upon. Even without the precise definition, many agree that accelerations characterize an important aspect of transient agility. For this reason an acceleration metric is suggested as one of the agility metrics that should be considered in a design. Of course other metrics, such as the derivative of acceleration (jerk) or functional agility metrics representing rates or displacements, can easily be accommodated in CRAFT.

Pitch acceleration, in the longitudinal axis, and stability axis roll acceleration in the lateral axis should be part of an agility metric set. For brevity, only the pitch acceleration metric is described in this paper. This pitch agility metric is an average pitch acceleration; it represents a blend of transient and functional agility characteristics. It is computed as peak pitch rate divided by the corresponding time to peak. At each design point the peak pitch rate is determined for a step input to the stabilator. To make the comparison correspond to the same motion at each design point, the steady-state pitch angle was adjusted to be the same. This required, in effect, a "gearing change" to be reflected in the closed-loop control distribution matrix. A gearing change was necessary because larger peak pitch rates occurred with low frequency placement of the short period pole. One reason for this is the superposition of short period and phugoid modes as the frequency of the short period pole is placed near the phugoid. Another

reason is from the increased gain required to achieve placement at higher frequencies. The higher gains reduced output magnitudes relative to the output magnitudes at lower gains. The overall result is that larger values of peak pitch rate, at lower frequency, dominate the metric plot. This can be seen by considering the state equation (3), with a simplified output equation given as

$$\dot{X} = A X + B_c U_c + B_p U_p \qquad X \in R^n \qquad (3)$$

$$Y = C X \qquad Y \in R^p \qquad (4)$$

$$U_c = GY \qquad U_c \in R^m \qquad (5)$$

The resulting closed-loop system produces a steady-state response, to a step pilot input U_p, given as

$$Y_{ss} = -C[A + B_c G C]^{-1} B_p U_p \qquad (6)$$

which shows reduced response levels as gain magnitude is increased. Thus, if maximum pitch rate were the only criteria, the contour plot would lead one to pick a low damping and a very low frequency for the short-period pole. However, this is clearly not the best design region since the time-to-peak is also very large and undesirable. To compensate for this, the average pitch acceleration metric is used, which becomes small if the peak time is large.

Flying Qualities Metrics

The fourth design objective area addresses pilot-in-the-loop issues. Flying qualities metrics are intended to help the designer assess the best tradeoff of pilot workload and performance. Figure 2 shows flying qualities specifications taken from Moorhouse-Moran, Mil-Std 1797A, and McDonnell Aircraft (ref. 19). These provide Level 1 regions for the short-period pole. The regions are presented, for this paper, in terms of short period frequency instead of the customary CAP parameter. The Level 2 region is not shown for clarity. The desirable regions for the short-period pole are much smaller in Moorhouse-Moran than the Mil-Std due to the restricted nature of the tasks considered by Moorhouse-Moran. These tasks were specifically tailored to fighter missions. This demonstrates the fluid nature of metrics as design requirements change and our knowledge base expands. Both the Moorhouse-Moran and the Mil-Std values are for the low angle of attack case. The McDonnell Aircraft work proposes desirable regions for fighters operating about 30□ angle of attack.

Control Synthesis Algorithm

In this study the control synthesis algorithm is Direct Eigenspace Assignment (DEA) taken from reference 20. This control synthesis technique provides a mechanism to determine measurement feedback control gains that produce an achievable eigenspace for the closed-loop system. It has been shown (ref. 21) that for a system that is observable and controllable with n states, m controls, and r measurements, one can exactly place r eigenvalues and m elements of their associated eigenvectors in the closed-loop system. DEA provides a mechanism to place q elements ($m<q<n$) of r eigenvectors associated with r eigenvalues through a least squares fit to the desired eigenvectors (see fig. 3).

System equations can be expressed as

$$\dot{X} = A X + B_c U_c + B_p U_p \qquad X \in R^n \qquad (7)$$

$$Y = C X + D_c U_c + D_p U_p \qquad Y \in R^p \qquad (8)$$

$$Z = M X + N_c U_c + N_p U_p \qquad Z \in R^r \qquad (9)$$

$$U_c = G Z \qquad U \in R^m \qquad (10)$$

Substituting the measurement equation for Z into the expression for U_c, the controller input can then be written as

$$U_c = G_x X + G_p U_p \qquad (11)$$

where

$$G_x = [I_m - G N_c]^{-1} G M$$

$$G_p = [I_m - G N_c]^{-1} G N_p$$

Thus the closed-loop system becomes

$$\dot{X} = [A + B_c G_x] X + [B_p + B_c G_p] U_p \qquad (12)$$

$$Y = [C + D_c G_x] X + [D_p + D_c G_p] U_p \qquad (13)$$

$$Z = [M + N_c G_x] X + [N_p + N_c G_p] U_p \qquad (14)$$

Spectral decomposition of the closed-loop system is given as

$$(A + B_c G_x) \nu_i = \lambda_i \nu_i \qquad i = 1,2,..., n \qquad (15)$$

This expression can be rearranged as

$$B_c G_x \nu_i = [I_n \lambda_i - A] \nu_i \qquad i = 1,2,..., n \qquad (16)$$

and defining

$$w_i = G_x \nu_i \qquad (17)$$

allows the closed-loop eigenvector from (16), in terms of w_i, to be written as

$$\nu_i = L_i w_i \qquad (18)$$

where

$$L_i = [I_n \lambda_i - A]^{-1} B_c.$$

The achievable eigenvector for the closed-loop system that reflects the desired eigenvalue and eigenvector specification can be written as

$$\nu_{ai} = L_{di} w_{ai} \qquad (19)$$

where

$$L_{di} = [I_n \lambda_{di} - A]^{-1} B_c.$$

If ν_{di} is substituted for ν_{ai} in equation (19), the result is a

weighted least squares problem for the unknown w_{ai}, for which the solution is

$$w_{ai} = [L_{di}^T Q_d L_{di}]^{-1} L_{di}^T Q_d \nu_{di} \qquad (20)$$

where Q_d is a weighting matrix to select q elements of the eigenvector to be specified. With w_{ai} determined, the feedback gains producing the achievable dynamics can be obtained from equation (17). After combining the column vectors for w_{ai} and ν_{ai} into matrices W and V, respectively, the gains are given by

$$G = W [M V + N_c W]^{-1} \qquad (21)$$

Further details of the derivation can be found in reference 20.

Design Example

To demonstrate the method, a single-point design example applying CRAFT to a 4th order linear, longitudinal model of a thrust-vectored F-18, trimmed at 30□ angle of attack, is presented. The design goal is to obtain desired longitudinal characteristics. The system states are velocity, angle of attack, pitch rate, and pitch attitude. Inputs are stabilator, thrust vectoring, and throttle. Full state feedback is assumed for convenience in the example, but this assumption is not required and does not reduce the effectiveness of CRAFT. For this example, only one metric from each of the four design objective areas is considered. In a more complete design many metrics from each design objective area would need to be considered. The design metrics for each of the four design areas are candidate metrics currently being studied and may be improved upon as experience is gained using the method. To completely cover the recommended range of possible pole locations, the desired short-period pole's frequency is varied from .1 rad/sec to 4.1 rad/sec and the damping ratio is varied from .2 to 1.8. This range is based on results from the McDonnell Aircraft simulation study at 30^o angle of attack (ref. 22).

In this example, the phugoid mode is specified to be Level 1 as given in MIl-Std 1797A, which requires a phugoid damping ratio of at least 0.04. A phugoid specification corresponding to a low α condition (α=5^o) should provide classical airplane response but to reach Level 1 this requires a slight increase in damping over the open-loop value of $(\zeta,\omega)_{ph}$ = (0.032, 0.068) to a closed-loop value of (0.04, 0.068). The phugoid and short-period eigenvectors are chosen from state-space models built up from transfer function descriptions that have the desired pole locations for both the short period and phugoid. Transfer function zeroes were chosen to be the same as the open-loop system. This procedure for defining eigenvectors and an optional procedure where the eigenvectors are required to maintain the same shape as the open-loop system at 5^o and 30^o angle of attack are discussed in Design Issues. These requirements are maintained over the ζ–ω space for each new short-period pole location. With the eigenspace specified, the feedback gains to achieve each short-period pole location were determined over the ζ–ω space of interest.

Once closed-loop systems are determined, metrics can be evaluated at each point over the ζ–ω space and a corresponding surface plotted to determine the metric sensitivity to pole location as well as the desirable regions to place the short period pole. Figures 4-7 each present one metric surface corresponding to each design objective area. Each figure shows a 3-D plot of the metric surfaces to enable easy visualization of the surface and a 2-D contour plot to highlight the desirable regions and enable the "overlaying" analysis. In these figures a gray scale is used to denote the gradient of desirability; dark shades correspond to undesirable values and progressively lighter shades correspond to increasing desirability. For example, lower values of GM (control power required) are the desirable regions and are shaded light.

Figure 4 presents a metric from the first design objective area (Control power) for this example. Figure 4b includes three contour lines superimposed at the .25, .5, and .75 levels, to highlight magnitude variation of the control power required metric. For this example, equation (1) is used in which all feedback gains are equally weighted. Plotted in this fashion the metric is a sensitivity measure indicating desirable regions and preferred directions to move the pole. The small gain metric values, in the region of low frequency and damping values, correspond to reduced gains (desirable values) and the higher values, in the high frequency and damping region, correspond to high gains and maximum required control power (undesirable values). This surface gives an indication of where, in terms of pole placement, the greatest control power demands will be placed on the control system. The most desirable region naturally tends to an area near the open-loop pole where no feedback is required. For this example, however, the gain metric does not go exactly to zero at the open-loop pole location since some feedback is still required to achieve the desired phugoid and eigenvector specification that does not correspond to the open-loop case.

Figure 5 shows a robustness measure based on an unstructured uncertainty model discussed in Design Approach. For this example the singular values were determined assuming the uncertainty was at the input. Figure 5a shows these singular values as a robustness metric over a range of frequency and damping. Figure 5b, giving the 2-D contours, shows an additional contour (shown as white lines) at the 0.5 level. As discussed before, for values of 0.5 or greater good robustness can be expected. This results in two fairly large desirable regions for frequencies below 2.0 rad/sec. The lighter regions of the plot correspond to the larger metric values and indicate the most desirable regions for short-period pole placement.

Figure 6 presents the airframe pitch agility metric as defined previously. Progressively lighter regions show the more desirable values of agility, i.e., greater pitch

acceleration. The 2-D contour plot has additional lines showing the 15, 25, 50, and 75 percent of peak value; for example, the contour line valued at 0.4 corresponds to 15% of the peak value that occurred over the ζ-ω space considered. Care must be used when comparing these metric values with measured instantaneous values of pitch acceleration. This is an average acceleration produced from a step input. In addition, the input was adjusted to provide the same steady-state pitch angle. Consequently, incorrect conclusions could result from a direct comparison with instantaneous values. Design experience will indicate the best values for this metric, however sensitivity information contained in the plot does provide an indicator of the best direction to move the poles for increasing agility.

The fourth design objective area covers pilot-in-the-loop requirements. A more detailed presentation of flying qualities specification for the short period mode is given in figure 7. This represents the more recently proposed McDonnell Aircraft results (ref. 22) for both gross acquisition and tracking combined into one simplified representation. The specification has been plotted in terms of frequency instead of CAP (n_Z/α = 2.5) for consistency among the metirc figures. Figure 7a shows the Level 1-2 and 2-3 boundaries for the 30□ angle of attack case. The desirable regions (Level 1 and Level 2) are clearly marked in the contour plot given in figure 7b. This is substantially different from low angle of attack recommended values shown in figure 2.

Figure 8 shows a final overlay plot of the desirable regions from each of the previous metric surfaces. Clearly, the best final design requires some judgement by the control designer, since the best region of each individual metric does not always overlap the others. This highlights the nature of control design requiring tradeoffs to be made to achieve a final overall design. An insightful choice is more readily made using CRAFT since the desirable regions and relative tradeoffs are graphically displayed. In this design problem, the more robust regions (large shaded areas) are on the left side of the figure, which fortunately, tends to be where the lower control power required area (solid contour lines) is located. A large portion of the Level 1 flying qualities region overlaps this area. One choice for this design might be to place the short period pole at lowest right-hand side of the Level 1 specification. This point should provide Level 1 flying qualities, good robustness to model error at the input, and relatively low gains. The pitch agility is maximized by moving to the lower right-hand corner of the plot. Greater values could be reached if the other design requirements are relaxed.

Design Issues

System scaling is an issue that arises when using DEA and CRAFT since it helps with interpretation of the eigenvectors. Scaling for this study was performed as follows:

$$X_S = TX \tag{22}$$

where

$$T = \text{diag}[1/V_o,\ 1/\alpha_o,\ 1/q_{max},\ 1/\theta_o] \tag{23}$$

and

V_o = 230 fps, q_{max} = 25 deg/sec, $\alpha_o = \theta_o$ = 30 deg.

which are trim values of the states except for q_{max} which is a nominal maximum pitch rate for this aircraft at the specified trim condition. Scaling leads to new system elements in equations (7-10); these new elements are

$$A_S = TAT^{-1},\ B_{cs} = TB_c,\ B_{ps} = TB_p,$$

$$C_S = CT^{-1},\ M_S = MT^{-1}$$

From a control designers point of view it is important to note that scaling the system affects the eigenvectors and gains that result from the design process. However, the system responses and eigenvalues are independent of system transformations. Therefore, interpretation of gains and eigenvectors must be done with knowledge of any scaling.

Another issue in the design process involves proper selection of both the eigenvalues and eigenvectors. Some guidance is needed for eigenvector selection, in particular. As explained above, the eigenvalue under study with CRAFT is simply specified over the ζ-ω space. The other eigenvalues need to be specified and desirable values for all the aircraft modes (at least for classical modes) are given in the Mil-Std 1797A. Desirable values for modes in the high angle of attack regime are still a matter of research.

Eigenvectors, on the other hand, need to be assembled by the designer. The eigenvector choice has a significant impact on feedback gains and unfortunately, there is not much guidance available for determining the best eigenvectors. Initially in this study it was assumed that the low angle of attack, open-loop model eigenvectors would be a reasonable place to start. These eigenvectors (with appropriate eigenvalues) represent classical airplane dynamics and might be desirable for the high angle of attack aircraft. Two problems arise with this choice. First, the eigenvectors are complex in order to match the corresponding complex eigenvalues. This presents a problem when it is desired to place poles with damping ratios greater than or equal to one. For ζ greater than or equal to one, the eigenvectors and eigenvalues become real. So the choice of eigenvectors must be real and this requires design information beyond that currently available (classical design specifications require complex eigenspace). The second problem is that the control power required to map the high angle of attack eigenspace into classical dynamics can be large. The gain metric shows maximum values two orders of magnitude greater with constant eigenvectors than that found using the transfer function build-up method used in this study. Figure 9 shows a comparison of gain metric for three choices of eigenvectors. The first two cases (figure 9a and 9b) are for fixed eigenvectors over the entire ζ-ω space. These contours were determined using

eigenvectors from the open-loop 5^o and 30^o angle of attack models, respectively; the last case (figure 9c) is for a variable eigenvector determined by the process described below. The maximum values of gain metric (gm_{max}) that occurred for each case are (for each figure): (9a) 134,340; (9b) 24,234; (9c) 604. These values typically occur at the extremes of the ζ-ω space considered and represent design points far from the region of interest; however, these values do indicate the relative merit of the three eigenvector choices. As seen in the figures, there is substantial change in the shape of the surface in addition to the height. As might be expected, choosing the desired eigenvector to be the same as the 30^o angle of attack case (fig. 9b) produces a bowl- shaped surface with the bottom of the bowl near the open-loop short-period pole. If the phugoid had been chosen to be exactly the open-loop value, the bottom would exactly correspond to the open-loop short-period pole. This case requires much lower gains, overall, than selecting ν_d to correspond to the 5^o angle of attack case (fig. 9a). The 5^o angle of attack case, besides having substantially higher gains, has drastically changed the shape of the surface; now the bottom occurs at the lowest frequency and highest damping considered (upper left-hand corner of the figure). Figure 9c demonstrates how lower gains, relative to the constant eigenvector case, can be achieved with the variable eigenvector approach. The shape of the surface again shows very low gains in the region of the open-loop pole, as expected.

The process of specifying eigenvectors in this study is based on a transfer function build-up of the desired input-output relationships and then transformation to a state space system to determine the eigenspace. The eigenvectors could be specified by the designer directly as linearly independent combinations of zeroes and ones. This is often seen in the literature when eigenspace assignment is used in an attempt to decouple responses of aircraft states. However, this does not respect some of the physical constraints of the aircraft. The choice of eigenvalue and eigenvector is closely related to specifying the placement of poles and zeroes in a transfer function representation. Transfer function zeroes are functions of aircraft physical characteristics, for example, $T_{\theta 2}$ is directly tied to $C_{L\alpha}$. Consequently, specifying nonaircraft-like values for these parameters may result in physically unachievable eigenvectors and large gains. Fortunately, DEA does allow a solution for the achievable eigenvectors that are as close to the desired eigenspace as possible, however there is no guarantee of small gains at the solution point. Very high gains imply the theoretically achievable eigenspace is not physically obtainable. The designer must work a tradeoff between achieving a desirable eigenspace and available control power. One way that shows promise in reducing the size of gains is to build up from aircraft transfer functions and specify only those parameters where appropriate.

This building process begins with an open-loop state space system of the aircraft states that can be written as

$$\dot{X} = A X + B U \tag{24}$$

$$Y = C X \tag{25}$$

This system can be transformed to transfer function form to obtain the poles, zeroes, and gains for all the input-output relationships. One should note that scaling and gain information will be lost in this transformation. In transfer function form it is easy to specify the desired poles. The zeroes also can be specified within limits that make sense for the aircraft. Note the design methodology will allow any desired specification to be made, however, the result is higher gains as the desired specification becomes less like the open-loop model. After appropriate specifications are made, the transformation back to state space can be performed. This step also causes a loss of information because the transformation back to state space is nonunique. The inputs and outputs of the system are the same, however. To reproduce the desired state space model, a simple transformation is performed. Given the nonphysical state space model obtained from transfer functions as

$$\dot{X}_n = A_n X_n + B_n U \tag{26}$$

$$Y = C_n X_n \tag{27}$$

It is possible to map back to the original state space model if C_n is invertible and the outputs Y are the desired physical states, X. Thus,

$$X_n = C_n^{-1} Y = C_n^{-1} X \tag{28}$$

Substituting this expression into the nonphysical state equation (24) produces

$$\dot{X} = C_n A_n C_n^{-1} X + C_n B_n U \tag{29}$$

which is the desired state equation.

Concluding Remarks

CRAFT, a combination of DEA and a graphical approach for representing control design metrics, has been introduced to provide greater insight into control design tradeoffs. CRAFT allows integration of multiple design goals in an efficient manner. The method allows the designer to use a building block approach to select or emphasize a particular required capability or general overall feature. In particular it should allow selection of dynamics that provide the greatest agility available while still satisfying appropriate levels of flying qualities, controlling system robustness, and still respecting the available control power. The approach allows MIMO design without requiring full-state feedback and by control of the closed-loop eigenspace flying qualities specifications can be incorporated into the design.

The CRAFT methodology provides insights into

tradeoffs for some common difficulties associated with eigenspace assignment such as large gains and a lack of robustness guarantees. These insights are provided in the form of a graphical display of the desirable regions for robustness and gain magnitudes. In addition, the sensitivity to pole placement is clearly displayed providing an indicator of the best directions to move poles for improvement. Caution is required by the user, however, to specify the dynamics (especially eigenvectors) with appropriate values to ensure acceptable gain magnitudes. In the final analysis, the overlay plot allows the designer to select acceptable levels of a variety of metrics as well as emphasize certain design goals, such as agility, to achieve any desired final effect.

References

1. Herbst, W.B. and Krogull, B.: Design for Air Combat. AIAA Paper 72-749, AIAA 4th Aircraft Design Flight Test and Operations Meeting, Los Angeles, California, August 7-9, 1972.

2. Eidetics International, Inc: Tactical Evaluation Of The Air-To-Air Combat Effectiveness Of Supermaneuverability. WRDC-TR-90-3035, June 1990.

3. McDonnell Aircraft Co., McDonnell Douglas Corp: Multi-System Integrated Control (MuSIC) Program. WRDC-TR-90-6001, June 1990.

4. Herbst, W.: Future Fighter Technologies. Journal of Aircraft, Vol. 17, No. 8, August 1980.

5. Hamilton, W.L. and Skow, A. M.: Operational Utility Survey: Supermaneuverability. AFWAL-TR-85-3020, September 1984.

6. Ogburn, M.E. et al.: Simulation Study of Flight Dynamics of a Fighter Configuration With Thrust-Vectoring Controls at Low Speeds and High Angles of Attack. NASA TP-2750, March 1988.

7. Nguyen, Luat T.: Flight Dynamics Research For Highly Agile Aircraft. SAE TP-892235, Aerospace Technology Conference and Exposition, Anaheim, CA, September 1989.

8. Foltyn, Robert W., et al.: Development of Innovative Air Combat Measures of Merit for Supermaneuverable Fighters. AFWAL-TR-87-3073, Eidetics, October 1987.

9. Hodgkinson, J., et al.: Relationships Between Flying Qualities, Transient Agility, and Operational Effectiveness of Fighter Aircraft. AIAA 88-4327, August 1988.

10. Phillips, William H.: Analysis of Effects of Interceptor Roll Performance and Maneuverability On Success of Collision-Course Attacks. NACA RM L58E27, August 1958.

11. McAtee, Thomas P.: Agility in Demand. Aerospace America, May 1988.

12. Tamrat, B.F.: Fighter Aircraft Agility Assessment Concepts and Their Implication on Future Agile Fighter Design. AIAA 88-4400, AIAA/AHS/ASEE Aircraft Design, Systems and Operations Meeting, Atlanta, September 7-9, 1988.

13. Skow, Andrew M., et al.: Advanced Fighter Agility Metrics, AIAA 85-1779, AFM Conference, Snowmass, August 1985.

14. Taylor, John H., et al.: Flight Test Validation of Advanced Agility Metrics for T-38 and F-4. USAF Contract F33615-85-C-0120, Eidetics TR 86-212, September 1986.

15. Skow, Andrew M., et al.: Transient Performance and Manevuerablity Measures of Merit for Fighter/Attack Aircraft, USAF Contract F33615-85-C-0120, Eidetics TR 86-201, January 1986.

16. Murphy, P. C.; Bailey, M. L.; Ostroff, A. J: Candidate Control Design Metrics For An Agile Fighter. NASA TM 4238, January 1991.

17. Mukhopadhyay, V. and Newsom, J. R. : A Multiloop System Stability Margin Study Using Matrix Singular Values. Journal of Guidance, Navigation, and Control, Vol. 8, No. 4, Sept.-Oct. 1984.

18. Bitten, R.: Qualitative and Quantitative Comparison of Government and Industry Agility Metrics. AIAA-89-3389-CP. A Collection of Technical Papers-AIAA Atmospheric Flight Mechanics Conference, Aug. 1989, pp. 368-376.

19. Riley, David R. and Drajeske, Mark H.: Relationships Between Agility Metrics and Flying Qualities. SAE Aerospace Atlantic Conference, 901003, April 1990.

20. Davidson, J. B. and Schmidt, D. K.: Flight Control Synthesis For Flexible Aircraft Using Eigenspace Assignment. NASA CR 178164, June 1986.

21. Srinathkumar, S.: Modal Control Theory and Application to Aircraft Lateral Handling Qualities Design, NASA TP-1234, June 1978.

22. Krekeler, Gregory C.; Wilson, David J.; Riley, David R.: High Angle-of-Attack Flying Qualities Criteria. AIAA 90-0219, 28th Aerospace Sciences Meeting, Reno, Nevada, January 1990.

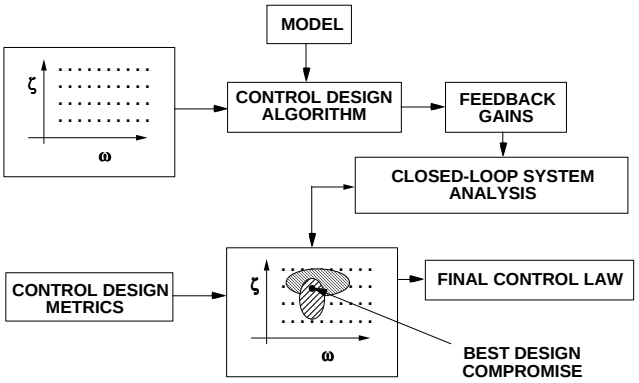

Figure 1. CRAFT control synthesis methodology

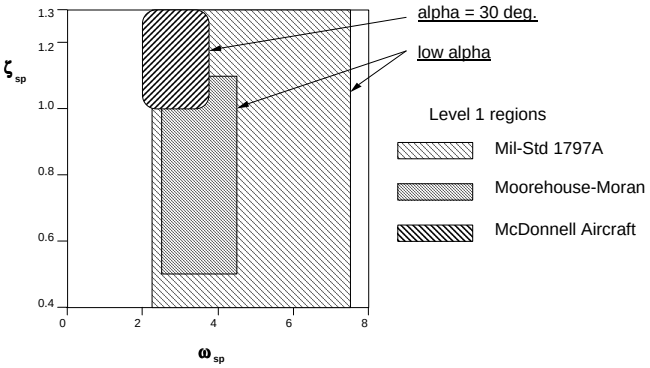

Figure 2. Level 1, longitudinal flying qualities

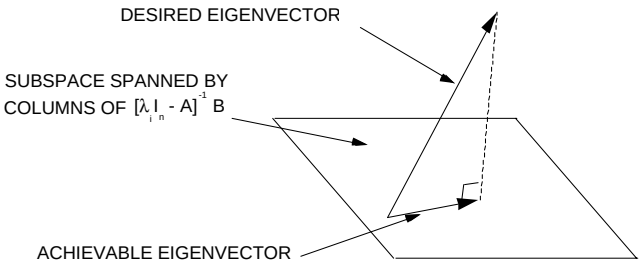

Figure 3. Achievable eigenvector obtained through DEA